

## **Mix design and early-age mechanical properties of ultra-high performance concrete**

\*Chao-Wei Tang<sup>1)</sup>

<sup>1)</sup> *Department of Civil Engineering & Geomatics, Cheng Shiu University,  
No. 840, Chengching Rd., Niasong District, Kaohsiung City, Taiwan  
R.O.C.*

<sup>1)</sup> [tangcw@gcloud.csu.edu.tw](mailto:tangcw@gcloud.csu.edu.tw)

### **ABSTRACT**

It is known from the literature that there are relatively few studies on the engineering properties of ultra-high performance concrete (UHPC) in early age. In fact, in order to ensure the safety of UHPC during construction and sufficient durability and long-term performance, it is necessary to explore the early behavior of UHPC. The test parameters (test control factors) investigated included the percentage of cement replaced by silica fume (SF), the percentage of cement replaced by ultra-fine silica powder (SFP), the amount of steel fiber (volume percent), and the amount of polypropylene fiber (volume percentage). The engineering properties of UHPC in the fresh mixing stage and at the age of 7 days were investigated. These properties include freshly mixed properties (slump, slump flow, and unit weight) and hardened mechanical properties (compressive strength, elastic modulus, flexural strength, and splitting tensile strength). Moreover, the effects of the experimental factors on the performance of the tested UHPC were evaluated by range analysis and variance analysis. The experiment results showed that the compressive strength of the C8 mix at the age of 7 days was highest of 111.5 MPa, and the compressive strength of the C1 mix at the age of 28 days was the highest of 128.1 MPa. In addition, the 28-day compressive strength in each experimental group increased by 13%-34% compared to the 7-day compressive strength. In terms of hardened mechanical properties, the performance of each experimental group was superior to that of the control group (without fiber and without additional binder materials), with considerable improvement, and the experimental group did not produce explosive or brittle damage after the test. Further, the flexural test process found that all test specimens exhibited deflection-hardening behavior, resulting in continued to increase carrying capacity after the first crack.

### **1. INTRODUCTION**

---

<sup>1)</sup> Professor

*The 2020 World Congress on  
The 2020 Structures Congress (Structures20)  
25-28, August, 2020, GECE, Seoul, Korea*

Construction materials are inextricably linked to structures because they affect the structural properties, construction methods and efficiency, maintenance, comfort and service life of the structures. Among various construction materials, Portland cement concrete is quite commonly used, and its composition includes cement, fine aggregates, coarse aggregates, water, and admixture. With the continuous development of concrete technology, various high-quality concrete products have been introduced, including high-strength concrete (HSC), high-performance concrete (HPC), fiber reinforced concrete (FRC), and ultra-high performance concrete (UHPC) (Okamura and Ozawa 1995, Petersson and Billberg 1996, Tattersall 1979, Al-Manaseer and Albert 1995, ACI Committee 544 1982, Song and Hwang, 2004, Swamy 1976, Hughes 1977, Velazco et al. 1980, Mindess and Bentur 1983, Khaloo and Kim 1996, Azmee and Shafiq 2018, Gosavi<sup>1</sup> and Awar 2018, He et al. 2018, Lai et al. 2018, Gu et al. 2018, Qu et al. 2018, Li et al. 2018, Mosaberpanah and Eren 2018, Rajkumar et al. 2018, Zhou et al. 2018, Larrard and Sedran 1994, Larrard and Sedran 2002, Sharma and Bansal 2019, Erdogdu et al. 2019).

According to the American Concrete Institute (ACI Committee 239 2012), UHPC is a cement-based concrete material with a minimum specified compressive strength of 150 MPa, which has specified durability, tensile ductility and toughness requirements. In addition, fibers are typically incorporated to meet specific requirements. In the 1990s, UHPC was originally called Reactive-Powder Concrete (RPC) because it contained only very fine materials (Graybeal 2014). In fact, the key factor in the production of UHPC is to improve the microscopic and macroscopic properties of its matrix composition to ensure mechanical homogeneity, maximum particle packing density and minimum size defects (Wille et al. 2011, Shi et al. 2015). Most publications directly give a mix proportion of UHPC, usually with a compressive strength greater than 120 MPa, but without any design procedures or explanations. The typical UHPC composition includes cement, supplementary cementitious materials (such as silica fume, fly ash and slag), fine sand, quartz or glass powder, superplasticizer, steel fiber and low water content (Abbas et al. 2016, Ghafari et al. 2015). As for the UHPC mix design, various methods have been proposed (Larrard and Sedran 1994, Larrard and Sedran 2002, Yu et al. 2014). For example, the Linear Packing Density Model, the Solid Suspension Model, the Compressible Packing Model, etc. proposed by Larrard and Sedran (Larrard and Sedran 1994, Larrard and Sedran 2002). These models all focus on the granular structure of UHPC.

Compared with ordinary concrete, the mix proportions of UHPC are characterized by low water-to-binder ratio, a large amount of fine-grained material, fine aggregate using only fine sand, high-dose superplasticizer and fiber material (Abbas et al. 2016). If compared with HPC, the proportion of cement used in UHPC is relatively high (800-1000 kg/m<sup>3</sup>) (Shi et al. 2015, Graybeal 2007). The literature shows that increasing the cement content in UHPC can increase its compressive strength; however, once the cement content exceeds its optimum value (about 1700 kg/m<sup>3</sup>), the compressive strength tends to decay due to the limited participation of the cement particles (Talebinejad et al. 2004). In the case of ordinary concrete, its failure is mainly caused by the damage of the Interfacial Transition Zone (ITZ) between the cement matrix and aggregates. Therefore, many UHPC ratios exclude coarse aggregates to reduce the presence of microcracks in the coarse aggregates and in the transitional regions between the matrix and the coarse

aggregates (Abbas et al. 2016, Alsalman et al. 2017). In addition, reducing the ITZ defect can reduce the total porosity of the matrix, thereby increasing the mechanical strength of the UHPC (Metha and Monteiro 2006). Since the composition of UHPC is blended with various cementitious materials, the coupling between thermal and mechanical characteristics of early-age UHPC is more important compared to that in ordinary concrete. Therefore, in order to ensure the safety of UHPC during construction, as well as enough durability and long-term performance, it is necessary to explore the early-age behavior of UHPC.

UHPC has enhanced mechanics and durability, which can reduce the size of structural members, save related materials, and reduce installation and labor costs, thus achieving economic benefits (Abbas et al. 2016, Alsalman et al. 2017, Burroughs et al. 2017, Pyo and Kim 2017, Pyo et al. 2016, Soliman and Tagnit-Hamou 2016). In fact, potential applications for UHPC include high-rise buildings, precast concrete engineering, structural and non-structural components. However, UHPC uses a large amount of cement, which not only affects production costs, but also consumes natural resources, resulting in a greenhouse effect (Burroughs et al. 2017). In addition, UHPC's initial cost is relatively high and may have a negative impact on the environment, limiting its widespread use in the construction industry. In view of this, this paper explores the UHPC mix design from the perspective of sustainable development, and replaces some cement with pozzolanic materials, and mixes steel fiber and polypropylene fiber, which not only has great help for energy saving and carbon reduction, but also improve its fresh properties, mechanical properties and durability. Moreover, the engineering properties of UHPC in the fresh mixing stage and at the age of 7 days were investigated. These properties include freshly mixed properties (slump, slump flow, and unit weight) and hardened mechanical properties (compressive strength, elastic modulus, flexural strength, and splitting tensile strength).

## **2. EXPERIMENTAL DETAILS**

### *2.1 Materials*

The materials used in the test included cement, silica fume, ultra-fine silica powder, fine aggregates, superplasticizers, viscous agent, steel fiber, and polypropylene fiber. A locally produced Type I Portland cement with a specific gravity of 3.15 and a fineness of 3400 cm<sup>2</sup>/g was used. The silica fume was locally manufactured with a specific gravity of 2.1 and a silicon dioxide content of 92.4%. The ultra-fine silica powder was purchased from abroad. Its specific gravity was 2.73 and an average particle diameter of 0.075 to 0.225 μm. The fine aggregate comprises two different sizes of quartz sand (i.e., Type 1 and Type 2). The physical properties and chemical composition of the fine granules are shown in Table 1, and the particle size distribution is shown in Table 2. The mixing ratio of fine aggregates is 80% of Type 1 and 20% of Type 2. Superplasticizers and viscous agent were local products (in accordance with the Chinese National Standards or the American Society for Testing Materials). The fibers used include steel fibers and polypropylene fibers, as shown in Fig. 1. The basic properties of these two fibers are shown in Table 3.

*The 2020 World Congress on  
The 2020 Structures Congress (Structures20)  
25-28, August, 2020, GECE, Seoul, Korea*

Table 1 Physical properties and chemical composition of fine aggregates

Type of Quartz Sand	Physical Properties		Chemical Composition		
	Specific Gravity (S.S.D)	Water absorption rate (%) (S.S.D)	SiO <sub>2</sub> (%)	Fe <sub>2</sub> O <sub>3</sub> (%)	Al <sub>2</sub> O <sub>3</sub> (%)
Type 1	2.65	≅0	99.82	0.014	0.033
Type 2	2.65	≅0	99.84	0.016	0.034

Table 2 Particle size distribution of fine aggregates

Sieve No. (ASTM E11-70)	Particle size ( $\mu\text{m}$ )	Percentage Retained (%)	
		Type 1	Type 2
20	850	0.04	-
30	600	20.15	-
40	425	67.83	-
50	300	11.81	-
60	250	-	0.05
70	212	0.17	13.69
100	150	-	36.55
140	106	-	32.39
200	75	-	12.73
270	53	-	3.61

Table 3 Basic properties of fibers

Type of fiber	Length (mm)	Diameter (mm)	Density (g/cm <sup>3</sup> )	Elastic Modulus (GPa)	Tensile Strength (MPa)	Melting Point (°C)
Steel Fibers	13	0.2	7.8	200	2000	-
Polypropylene Fibers	12	0.05	0.9	-	300	165



(a) Steel fibers



(b) Polypropylene fibers

Fig. 1 Fibers appearance

## 2.2 Experimental design

There are four test parameters (test control factors), including: the percentage of cement replaced by silica fume (SF), the percentage of cement replaced by ultra-fine silica powder (SFP), the amount of steel fiber (volume percent), and the amount of polypropylene fiber (volume percentage). Table 4 lists the levels of each test parameter

*The 2020 World Congress on  
The 2020 Structures Congress (Structures20)  
25-28, August, 2020, GECE, Seoul, Korea*

of the concrete and its performance parameters. The general full-factor design considers all combinations of factors, resulting in a large experimental workload (Fisher 1925). In contrast, the Taguchi method uses orthogonal arrays for experimental design, which can greatly reduce the number of trials (Taguchi 1987). In view of this, this paper uses the Taguchi method to plan experimental design. As shown in Table 5, an orthogonal array  $L_9(3^4)$  was adopted for UHPC, which consisted of four controllable three-level factors.

**Table 4 Parameters and design levels for UHPC**

Parameter (Experimental Control Factor)	Levels of Parameter			Performance Parameter
	1	2	3	
Percentage of Cement Replaced by SF, A (%)	17.4	18.7	20.0	Unit Weight, Slump, Slump Flow, Compressive Strength, Elastic Modulus, Flexural Strength, Splitting Strength
Percentage of Cement Replaced by SFP, B (%)	2.2	2.7	3.2	
Amount of PP (Volume Percent), C (%)	0.03	0.06	0.09	
Amount of Steel Fiber (Volume Percentage), D (%)	0.5	0.75	1.0	

Notes: SF=silica fume; SFP=ultra-fine silica powder; PP=polypropylene fiber.

**Table 5  $L_9(3^4)$  orthogonal array for UHPC**

Experiment Number	Parameter (Level)			
	Percentage of Cement Replaced by SF, A (%)	Percentage of Cement Replaced by SFP, B (%)	Amount of PP (Volume Percent), C (%)	Amount of Steel Fiber (Volume Percentage), D (%)
C1	17.4(1)	2.2(1)	0.03(1)	0.5(1)
C2	17.4(1)	2.7(2)	0.06(2)	0.75(2)
C3	17.4(1)	3.2(3)	0.09(3)	1.0(3)
C4	18.7(2)	2.2(1)	0.06(2)	1.0(3)
C5	18.7(2)	2.7(2)	0.09(3)	0.5(1)
C6	18.7(2)	3.2(3)	0.03(1)	0.75(2)
C7	20.0(3)	2.2(1)	0.09(3)	0.75(2)
C8	20.0(3)	2.7(2)	0.03(1)	1.0(3)
C9	20.0(3)	3.2(3)	0.06(2)	0.5(1)

Note: \* The numbers in parentheses indicate the level of the factor; SF=silica fume; SFP=ultra-fine silica powder; PP=polypropylene fiber.

### *2.3 Mix proportions and casting of specimens*

According to the orthogonal arrays, namely  $L_9(3^4)$ , the mix proportions of the UHPC are listed in Table 6. In addition to the experimental group (No. C1-C9), pure concrete was also used as the control group (No. C0) of the experiment, that is, no fiber and cementitious materials (silica fume and ultra-fine silica powder) were added for comparison and discussion. Before mixing, the fine aggregates were treated to a dry state because their water absorption rate approached zero. The cementitious material and fine aggregates were then dry blended uniformly in minutes, followed by the addition of water, fibers, superplasticizer, and viscous agent. Once the mixture was uniformly mixed, the fresh properties of each mixture were measured and recorded. Afterward, concrete specimens required for each test were cast and an external vibrator was used to ensure that the specimens were sufficiently compacted. The compressive strength and elastic modulus test were cylindrical specimens with a diameter of 100 mm and a height

*The 2020 World Congress on  
The 2020 Structures Congress (Structures20)  
25-28, August, 2020, GECE, Seoul, Korea*

of 200 mm. The splitting strength test used a cylindrical specimen with a diameter of 150 mm and a height of 300 mm. For the flexural strength test, a prism sample having a length of 360 mm, a width of 100 mm, and a thickness of 100 mm was used. After casting the specimens, they were covered with polyethylene sheets for 24 hours overnight. The demolding operation was then carried out and each specimen was placed in a laboratory water bath until the day before the mechanical test.

**Table 6 Mix proportions of UHPC**

Mix No.	W/B	W (kg/m <sup>3</sup> )	C (kg/m <sup>3</sup> )	SF (kg/m <sup>3</sup> )	SFP (kg/m <sup>3</sup> )	SP (kg/m <sup>3</sup> )	VA (kg/m <sup>3</sup> )	PP (kg/m <sup>3</sup> )	Steel Fiber (kg/m <sup>3</sup> )	FA (kg/m <sup>3</sup> )
C0	0.20	196	1005	0	0	26	1	0	0	1286
C1	0.20	187	774	167	21	25	1	0.3	39	1231
C2	0.20	187	767	167	26	25	1	0.5	59	1228
C3	0.20	186	760	166	31	25	1	0.8	78	1225
C4	0.20	186	756	179	21	25	1	0.5	78	1223
C5	0.20	187	754	180	26	25	1	0.8	39	1229
C6	0.20	186	748	179	31	25	1	0.3	59	1225
C7	0.20	186	744	191	21	25	1	0.8	59	1223
C8	0.20	186	737	191	26	25	1	0.3	78	1220
C9	0.20	186	736	192	31	25	1	0.5	39	1226

Notes: W/B= water-binder ratio; W=water; C= cement; SF=silica fume; SFP=ultra-fine silica powder; SP= superplasticizers; VA= viscous agent; PP= polypropylene fiber; FA= fine aggregate.

#### 2.4 Test methods and data analysis

The tests of unit weight, slump, slump flow, compressive strength, elastic modulus, splitting tensile strength, and flexural strength of UHPC were carried out according to ASTM C138, ASTM C143, ASTM C1611, ASTM C39, ASTM C469, ASTM C496 and ASTM C78 standards (ASTM C138/C138M-17a 2017, ASTM C143/C143M-15a 2015, ASTM C1611/C1611M-18 2018, ASTM C39/C39M-18 2018, ASTM C469/C469M-14 2014, ASTM C496/C496M-11 2004, ASTM C78/C78M-18 2018), respectively.

When the Taguchi experimental design method is applied, the deviation between the experimental value and the expected value is usually calculated by a so-called loss function. In short, the loss function can be used to measure performance characteristics that deviate from the expected value. Conventionally, the value of the loss function is usually converted to a signal-to-noise ratio (S/N) ratio ( $\eta$ ) (Montgomery 2005). In general, there are three types of performance characteristics such as the following (Montgomery 2005):

$$\text{The smaller-the better: } \eta = -10 \times \log_{10}(MSD) = -10 \times \log_{10}\left(\frac{1}{n} \sum_{i=1}^n y_i^2\right) \quad (1)$$

$$\text{The larger-the better: } \eta = -10 \times \log_{10}(MSD) = -10 \times \log_{10}\left(\frac{1}{n} \sum_{i=1}^n \frac{1}{y_i^2}\right) \quad (2)$$

$$\text{The nominal-the better: } \eta = -10 \times \log_{10}(MSD) = -10 \times \log_{10}\left(\frac{1}{n} \sum_{i=1}^n (y_i - y_0)^2\right) \quad (3)$$

The 2020 World Congress on  
**The 2020 Structures Congress (Structures20)**  
 25-28, August, 2020, GECE, Seoul, Korea

where  $MSD$  = the mean squared deviation around the target value;  $n$  = the number of repetitions or observations;  $y_i$  = the observed data; and  $y_0$  = the nominal value desired.

In this study, the observed values of the mechanical properties of the UHPC were set to a maximum level. In addition, the optimization of the observations was further detected by analysis of variance. This was mainly achieved by separating the total variability of the  $S/N$  ratios into contributions of each of the process parameters and the error (Neville 1994).

### 3. RESULTS AND DISCUSSION

#### 3.1 Properties of fresh UHPC

The results of the fresh properties of the control group (C0) and the experimental group (C1-C9), including the slump, slump flow, and unit weight, are shown in Table 7. Moreover, the corresponding  $S/N$  ratio of the experimental group is shown in Table 7. In addition, Table 8 lists the mean  $S/N$  ratio at each level of the experimental control factors for various performance parameters. On the other hand, the results of the variance analysis of various performance parameters are given in Table 9. In addition, the  $F$  values were obtained with a 95% level of confidence, and the percentage contribution of each parameter was also calculated.

Table 7 Experimental results and  $S/N$  ratio of UHPC

Mix No.	Experimental Results (MPa)			$S/N$ Ratio (dB)		
	Slump (cm)	Slump Flow (cm)	Unit Weight (kg/m <sup>3</sup> )	Slump	Slump Flow	Unit Weight
C0	26.2	69.0	2318.3	-	-	-
C1	25.5	53.0	2263.4	28.13	34.49	67.10
C2	25.5	51.0	2279.6	28.13	34.15	67.16
C3	25.5	49.0	2267.6	28.13	33.80	67.11
C4	25.7	54.0	2316.2	28.20	34.65	67.30
C5	26.2	58.0	2237.3	28.37	35.27	66.99
C6	26.0	49.0	2274.6	28.30	33.80	67.14
C7	25.5	53.0	2288.7	28.13	34.49	67.19
C8	25.0	51.0	2308.5	27.96	34.15	67.27
C9	26.0	53.0	2250.7	28.30	34.49	67.05

Table 8  $S/N$  ratio response table of Fresh UHPC

Performance Parameter	Parameter (Experimental Control Factor)	Mean $S/N$ Ratio ( $\eta$ , Unit: dB)			Delta (Max. $\eta$ - Min. $\eta$ )	Rank
		Level 1	Level 2	Level 3		
Slump	Percentage of Cement Replaced by SF, A (%)	28.13	28.29	28.13	0.158	2
	Percentage of Cement Replaced by SFP, B (%)	28.15	28.15	28.24	0.091	3
	Amount of PP (Volume Percent), C (%)	28.13	28.21	28.21	0.080	4
	Amount of Steel Fiber (Volume Percentage), D (%)	28.27	28.19	28.10	0.169	1
Slump Flow	Percentage of Cement Replaced by SF, A (%)	34.15	34.57	34.37	0.427	3
	Percentage of Cement Replaced by SFP, B (%)	34.54	34.52	34.03	0.509	2
	Amount of PP (Volume Percent), C (%)	34.15	34.43	34.52	0.372	4
	Amount of Steel Fiber (Volume Percentage), D (%)	34.75	34.15	34.20	0.600	1
Unit Weight	Percentage of Cement Replaced by SF, A (%)	67.12	67.14	67.17	0.047	4
	Percentage of Cement Replaced by SFP, B (%)	67.19	67.14	67.10	0.096	2
	Amount of PP (Volume Percent), C (%)	67.17	67.17	67.10	0.067	3
	Amount of Steel Fiber (Volume Percentage), D (%)	67.05	67.16	67.22	0.179	1

Table 9 Variance analysis and *F* test for Fresh UHPC

Performance Parameter	Parameter (Experimental Control Factor)	Sum of Square ( $SS_2$ )	Degree of Freedom	Variance ( $MS_2$ )	<i>F</i> Value ( $F_2$ )	Percentage Contribution ( $P_2$ )
Slump	Percentage of Cement Replaced by SF, A (%)	0.05	3	0.02	3.92	30.39
	Percentage of Cement Replaced by SFP, B (%)	0.02	3	0.01	1.29	3.03
	Amount of PP (Volume Percent), C (%)	0.01	3	0.00	1.00	41.68
	Amount of Steel Fiber (Volume Percentage), D (%)	0.04	3	0.01	3.39	24.89
	All Other/Error	0.01	3	0.00	–	–
	Total	0.12	12	0.04	–	100.00
Slump Flow	Percentage of Cement Replaced by SF, A (%)	0.27	3	0.09	1.21	2.84
	Percentage of Cement Replaced by SFP, B (%)	0.50	3	0.17	2.22	16.59
	Amount of PP (Volume Percent), C (%)	0.23	3	0.08	1.00	54.45
	Amount of Steel Fiber (Volume Percentage), D (%)	0.66	3	0.22	2.92	26.12
	All Other/Error	0.23	3	0.08	–	–
	Total	1.66	12	0.55	–	100.00
Unit Weight	Percentage of Cement Replaced by SF, A (%)	0.00	3	0.00	1.00	0.00
	Percentage of Cement Replaced by SFP, B (%)	0.01	3	0.00	4.15	13.81
	Amount of PP (Volume Percent), C (%)	0.01	3	0.00	2.72	25.09
	Amount of Steel Fiber (Volume Percentage), D (%)	0.05	3	0.02	14.92	61.10
	All Other/Error	0.00	3	0.00	–	–
	Total	0.08	12	0.03	–	100.00

### 3.1.1 Slump

As can be seen from Table 7, the slump of each series was between 25.0 and 26.2 cm, and the average value of the experimental group was 25.65 cm. Most of the mixtures can reach 25.5 cm or more, and all have excellent workability. Among them, the slump of the C8 mix was the smallest (25.0 cm), and the slump of the C0 and C5 mixes was the largest (26.2 cm). Because the experimental design was orthogonal, the effect of each experimental control factor at different levels could be clearly separated. Taking the percentage of cement replaced by silica fume as an example, the mean *S/N* ratio at levels 1, 2, and 3 were calculated by averaging the *S/N* ratios of experiments 1–3, 4–6, and 7–9, respectively. For other experimental control factors, the average *S/N* ratio for each level was calculated in a similar manner. The delta column in Table 8 shows the difference between the maximum and minimum values of the mean *S/N* ratio from Level 1 to Level 3. In theory, the importance can be evaluated by the delta value of each factor—the larger the delta value is, the greater the influence of the level of change of the factor on the performance parameter and the more important the factor is. As shown in Equation (2), the larger the *S/N* ratio is, the smaller the variance in slump value around the desired value is (i.e., the larger—the better). Fig. 2 shows the *S/N* ratio response graph for the slump. It can be seen from Fig. 2 that as the amount of steel fiber increased, the *S/N* ratio tended to decrease. In other words, the value of the slump was reduced. From the analysis results of Table 8 and Fig. 2, it can be concluded that the amount of steel fiber was the significant factor affecting slump; the maximum response occurred in 0.5% (volume percentage). For the variance analysis results of the slump, as shown in Table 9, the amount of polypropylene fiber was the most important factor affecting the slump of the concrete. The percentage contributions of these factors were as follows: the amount of polypropylene fiber (41.68%), the percentage of cement replaced by silica fume (30.39%), and the amount of steel fiber (24.89%). Therefore, based on the analysis results of the above range analysis and variance analysis, the optimal combination level of the experimental control factors for achieving maximum slump is  $A_2B_3C_2D_1$ .

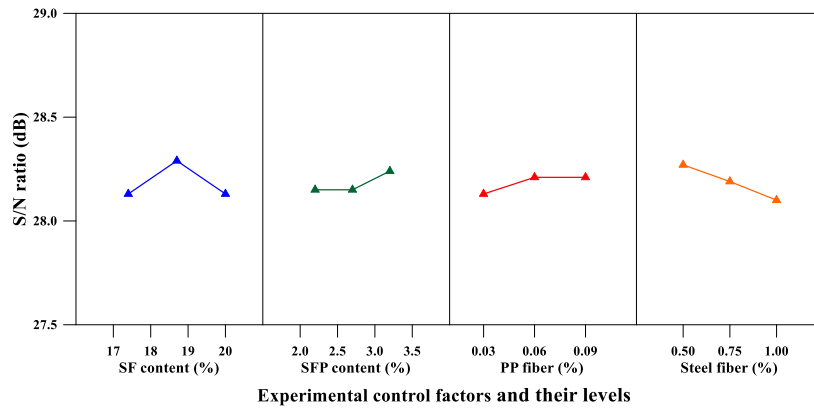


Fig. 2 S/N ratio response graph of the slump values of UHPC

### 3.1.2 Slump flow

Table 7 shows that the slump flow was between 49 and 69 cm. In the experimental group, the slump flow of the C3 and C6 mixes was the smallest (49 cm), while the slump flow of the C5 mix was the largest (58 cm). Compared with the control group, the slump flow of the C3 and C6 mixes was significantly lower. The reason is that the fibers were not easily mixed during concrete mixing and were less likely to be uniformly dispersed in the paste. Furthermore, due to the local agglomeration of steel fibers in the concrete, the flow of the aggregates was hindered, resulting in reduced workability; the polypropylene fibers were formed to have a large specific surface area due to their very slenderness. This led to an increase in the consistency of the concrete, which degraded the workability. From the analysis results of Table 8 and Fig. 3, it can be concluded that the amount of steel fiber was the significant factor affecting slump flow; the maximum response occurred was at the lowest level of the amount of steel fiber. For the variance analysis results of slump flow, as shown in Table 9, the amount of polypropylene fiber was the most important factor affecting the slump flow of the concrete. The percentage contributions of these factors were as follows: the amount of polypropylene fiber (54.45%), the amount of steel fiber (26.12%), and the percentage of cement replaced by ultra-fine silica powder (16.59%). According to the analysis results of the above range analysis and variance analysis, the optimal combination level of the experimental control factors for achieving maximum slump flow is  $A_2B_1C_3D_1$ .

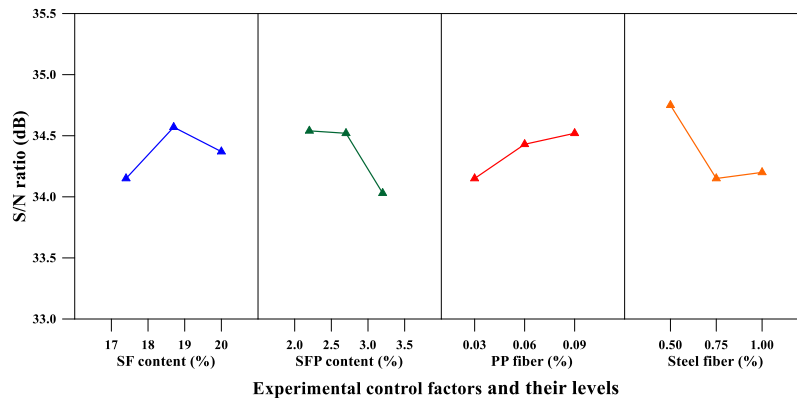


Fig. 3 S/N response graph of the slump flow values of UHPC

### 3.1.3 Unit weight

On the other hand, Table 7 also shows the unit weight test results for each series of concrete. The unit weight was between 2237.3 and 2318.3 kg/m<sup>3</sup>, of which the unit weight of the C5 mix was the smallest (2237.3 kg/m<sup>3</sup>), and the unit weight of the C0 mix was the largest (2318.3 kg/m<sup>3</sup>). Overall, the unit weight ratio between the experimental group and the control group ranged from 0.965 to 0.999, with no significant difference from each other. In addition, Fig. 4 shows the S/N ratio response graph for unit weight. It can be seen from Fig. 4 that as the amount of steel fiber increased, the S/N ratio tended to increase. In other words, the value of the unit weight was increased. From the analysis results of Table 8 and Fig. 4, it can be concluded that the amount of steel fiber was the significant factor affecting unit weight; the maximum response occurred in 1.0% (volume percentage). For the variance analysis results of unit weight, as shown in Table 9, the amount of steel fiber was the most important factor affecting the unit weight of the concrete. The percentage contributions of these factors were as follows: the amount of steel fiber (61.10%), the amount of polypropylene fiber (25.09%), and the percentage of cement replaced by ultra-fine silica powder (13.81%). According to the analysis results of the above range analysis and variance analysis, the optimal combination level of the experimental control factors for achieving maximum unit weight is A<sub>3</sub>B<sub>1</sub>C<sub>1</sub>D<sub>3</sub>.

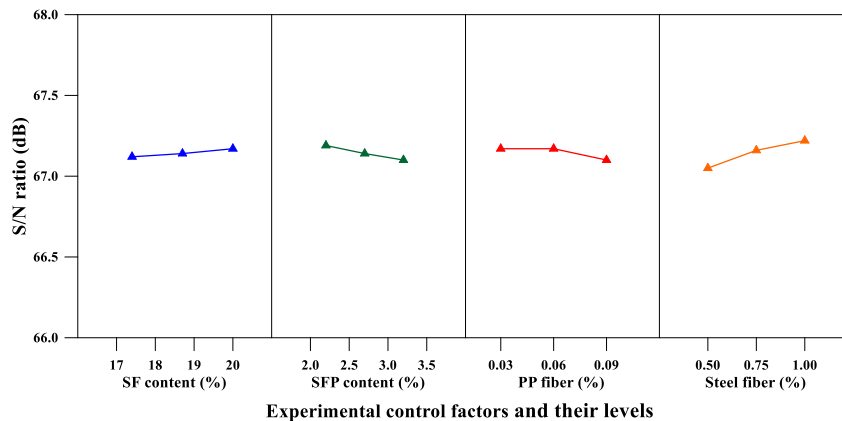


Fig. 4 S/N ratio response graph of the unit weight values of UHPC

### 3.2 Properties of hardened UHPC

The 7-day results of the hardened properties of the control group (C0) and the experimental group (C1-C9), including the compressive strength, elastic modulus, flexural strength, and splitting strength, are shown in Table 10. Further, the corresponding S/N ratio of the experimental group is also shown in Table 10. In addition, Table 11 lists the mean S/N ratio at each level of the experimental control factors for various performance parameters. On the other hand, the results of the variance analysis of various performance parameters are given in Table 12. In addition, the F values were obtained with a 95% level of confidence, and the percentage contribution of each parameter was also calculated.

The 2020 World Congress on  
**The 2020 Structures Congress (Structures20)**  
 25-28, August, 2020, GECE, Seoul, Korea

Table 10 Experimental results and S/N ratio of hardened UHPC

Mix No.	7-day Experimental Results				S/N Ratio (dB)			
	$f'_c$ (MPa)	$E_c$ (GPa)	$f_r$ (MPa)	$f_s$ (MPa)	$f'_c$	$E_c$	$f_r$	$f_s$
C0	81.6	32.3	6.6	4.4	-	-	-	-
C1	95.7	34.9	12.6	7.3	39.62	30.86	22.01	17.27
C2	100.0	38.9	12.9	7.3	40.00	31.80	22.21	17.27
C3	94.0	38.9	18.0	9.4	39.46	31.80	25.11	19.46
C4	107.0	37.2	15.1	9.6	40.59	31.41	23.58	19.65
C5	94.3	38.8	9.3	8.2	39.49	31.78	19.37	18.28
C6	97.8	33.9	14.7	10.5	39.81	30.60	23.35	20.42
C7	95.6	35.4	12.2	8.9	39.61	30.98	21.73	18.99
C8	111.5	36.9	12.7	10.8	40.95	31.34	22.08	20.67
C9	102.4	35.5	12.7	7.9	40.21	31.00	22.08	17.95

Note:  $f'_c$ =compressive strength;  $E_c$ = elastic modulus;  $f_r$ = flexural strength;  $f_s$ = splitting strength.

Table 11 S/N ratio response table of hardened UHPC

Performance Parameter	Parameter (Experimental Control Factor)	Mean S/N Ratio ( $\eta$ , Unit: dB)			Delta (Max. $\eta$ - Min. $\eta$ )	Rank
		Level 1	Level 2	Level 3		
Compressive Strength	Percentage of Cement Replaced by SF, A (%)	39.69	39.96	40.25	0.560	3
	Percentage of Cement Replaced by SFP, B (%)	39.94	40.15	39.83	0.320	4
	Amount of PP (Volume Percent), C (%)	40.12	40.26	39.52	0.744	1
	Amount of Steel Fiber (Volume Percentage), D (%)	39.77	39.81	40.33	0.560	2
Elastic Modulus	Percentage of Cement Replaced by SF, A (%)	31.48	31.26	31.11	0.376	4
	Percentage of Cement Replaced by SFP, B (%)	31.08	31.64	31.14	0.556	2
	Amount of PP (Volume Percent), C (%)	30.93	31.40	31.52	0.585	1
	Amount of Steel Fiber (Volume Percentage), D (%)	31.21	31.13	31.52	0.389	3
Flexural Strength	Percentage of Cement Replaced by SF, A (%)	23.11	22.10	21.96	1.148	3
	Percentage of Cement Replaced by SFP, B (%)	22.44	21.22	23.51	2.290	2
	Amount of PP (Volume Percent), C (%)	22.48	22.62	22.07	0.555	4
	Amount of Steel Fiber (Volume Percentage), D (%)	21.15	22.43	23.59	2.436	1
Splitting Strength	Percentage of Cement Replaced by SF, A (%)	18.00	19.45	19.20	1.450	2
	Percentage of Cement Replaced by SFP, B (%)	18.63	18.74	19.28	0.646	4
	Amount of PP (Volume Percent), C (%)	19.45	18.29	18.91	1.165	3
	Amount of Steel Fiber (Volume Percentage), D (%)	17.83	18.89	19.93	2.094	1

Table 12 Variance analysis and F test for hardened UHPC

Performance Parameter	Parameter (Experimental Control Factor)	Sum of Square (SS <sub>2</sub> )	Degree of Freedom	Variance (MS <sub>2</sub> )	F Value (F <sub>2</sub> )	Percentage Contribution (P <sub>2</sub> )
Compressive Strength	Percentage of Cement Replaced by SF, A (%)	0.47	3	0.16	2.98	14.48
	Percentage of Cement Replaced by SFP, B (%)	0.16	3	0.05	1.00	0.00
	Amount of PP (Volume Percent), C (%)	0.94	3	0.31	5.92	65.39
	Amount of Steel Fiber (Volume Percentage), D (%)	0.59	3	0.20	3.75	20.13
	All Other/Error	0.16	3	0.05	-	-
	Total	2.16	12	0.72	-	100.00
Elastic Modulus	Percentage of Cement Replaced by SF, A (%)	0.21	3	0.07	1.00	0.00
	Percentage of Cement Replaced by SFP, B (%)	0.57	3	0.19	2.63	21.79
	Amount of PP (Volume Percent), C (%)	0.58	3	0.19	2.69	75.94
	Amount of Steel Fiber (Volume Percentage), D (%)	0.25	3	0.08	1.17	2.27
	All Other/Error	0.21	3	0.07	-	-
	Total	1.61	12	0.54	-	100.00
Flexural Strength	Percentage of Cement Replaced by SF, A (%)	2.36	3	0.79	4.75	9.47
	Percentage of Cement Replaced by SFP, B (%)	7.88	3	2.63	15.86	37.58
	Amount of PP (Volume Percent), C (%)	0.50	3	0.17	1.00	10.12
	Amount of Steel Fiber (Volume Percentage), D (%)	8.91	3	2.97	17.93	42.83
	All Other/Error	0.50	3	0.17	-	-
	Total	19.64	12	6.55	-	100.00
Splitting Strength	Percentage of Cement Replaced by SF, A (%)	3.61	3	1.20	5.00	22.32
	Percentage of Cement Replaced by SFP, B (%)	0.72	3	0.24	1.00	0.00
	Amount of PP (Volume Percent), C (%)	2.04	3	0.68	2.82	32.48
	Amount of Steel Fiber (Volume Percentage), D (%)	6.58	3	2.19	9.10	45.20
	All Other/Error	0.72	3	0.24	-	-
	Total	12.95	12	4.32	-	100.00

### 3.2.1 Compressive strength

In general, the use of pozzolanic materials will affect the development of early-age compressive strength of UHPC, depending on its type, amount of addition, mineral composition, particle shape and fineness, and pozzolanic activity. It can be seen from Table 10 that the 7-day compressive strength of the UHPC mixtures was between 81.6 and 111.5 MPa. Among them, the C0 mix had the lowest compressive strength (81.6 MPa), and the C8 mix had the highest compressive strength (111.5 MPa). This result shows that the incorporation of pozzolanic materials can enhance the early-age compressive strength of UHPC, and the percentage of improvement was between 15.2% and 36.6%. Moreover, Table 13 shows the percentage of 28-day compressive strength achieved by the UHPC mixture at seven days. For the C8 mix containing large amounts of silica fume, its 7-day compressive strength was 89% of 28-day compressive strength. As for the C0 mix containing large amounts of cement, its 7-day compressive strength was 91% of 28-day compressive strength.

Table 13 Development of compressive strength

Mix No.	$f'_{c-7d}$ (MPa)	$f'_{c-28d}$ (MPa)	$f'_{c-7d}/f'_{c-28d}$
C0	81.6	90.0	0.91
C1	95.7	128.1	0.75
C2	100.0	113.7	0.88
C3	94.0	119.8	0.78
C4	107.0	127.0	0.84
C5	94.3	124.9	0.76
C6	97.8	121.6	0.80
C7	95.6	123.6	0.77
C8	111.5	125.8	0.89
C9	102.4	120.2	0.85

Note:  $f'_{c-7d}$  = 7-day compressive strength;  $f'_{c-28d}$  = 28-day compressive strength.

Fig. 5 shows the S/N ratio response graph for compressive strength. It can be seen from Fig. 5 that as the amount of silica fume and steel fiber increased, the S/N ratio tended to increase. In other words, the value of the compressive strength was increased. From the analysis results of Table 11 and Fig. 5, it can be concluded that the amount of polypropylene fiber was the significant factor affecting compressive strength; the maximum response occurred in 0.06% (volume percentage). For the variance analysis results of compressive strength, as shown in Table 12, the amount of polypropylene fiber was the most important factor affecting the compressive strength of the concrete. The percentage contributions of these factors were as follows: amount of polypropylene fiber (65.39%), amount of steel fiber (20.13%), and percentage of cement replaced by silica fume (14.48%). According to the analysis results of the above range analysis and variance analysis, the optimal combination level of the experimental control factors for achieving maximum compressive strength is A<sub>3</sub>B<sub>2</sub>C<sub>2</sub>D<sub>3</sub>.

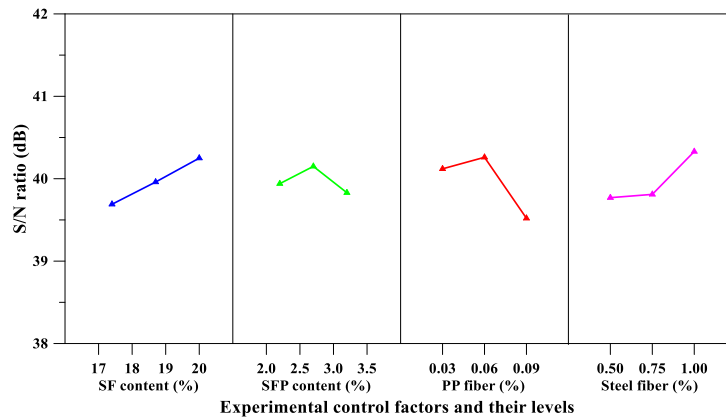


Fig. 5 S/N ratio response graph of the compressive strength values of UHPC

### 3.2.2 Elastic modulus

Fig. 6 shows the stress-strain curve of each UHPC mix at 7 days of age. As can be seen from Fig. 6, the initial slope of the ascending branches of the stress-strain curve exhibited a linear relationship before reaching the maximum stress. According to ASTM C469, the elastic modulus of the specimen was obtained from the stress-strain curve. It can be seen from Table 10 that the 7-day elastic modulus of the UHPC mixtures was between 32.3 and 38.9 GPa. Among them, the C0 mix had the lowest elastic modulus (32.3 GPa), and the C2 and C3 mixes had the highest elastic modulus (38.9 GPa). However, in the experimental group, there was no significant difference in the elastic modulus of each specimen. Moreover, the age of concrete at the time of testing was not found significantly to affect the modulus of elasticity. Especially, for the C2-C6 mixtures, their  $E_{c-7D}/E_{c-28D}$  value was between 0.98-1.0, as shown in Table 14. This is because the early concrete modulus of elasticity developed very rapidly compared to the compressive strength (Nehdi and Soliman 2011). Myers (1999) pointed out that about 90% or more of the elastic modulus value is achieved within the first 24 h after casting.

Fig. 7 shows the S/N ratio response graph for elastic modulus. It can be seen from Fig. 7 that as the amount of polypropylene fiber increased, the S/N ratio tended to increase. According to the average S/N ratio of the elastic modulus parameters of Table 11 and the elastic modulus S/N response diagram of Fig. 7, the polypropylene fiber content was an important factor affecting the elastic modulus of UHPC, and the maximum response was on the third level of the polypropylene fiber content. Further, the results of the analysis of variance for elastic modulus are given in Table 12. It can also be confirmed from Table 12 that the polypropylene fiber content is the most important factor affecting the elastic modulus of the concrete. The percentage contributions of these factors were as follows: the amount of polypropylene fiber (75.94%) and the percentage of cement replaced by ultra-fine silica powder (21.79%). According to the analysis results of the above range analysis and variance analysis, the optimal combination level of the experimental control factors for achieving maximum elastic modulus is A<sub>1</sub>B<sub>2</sub>C<sub>3</sub>D<sub>3</sub>.

Table 14 Development of elastic modulus

Mix No.	$E_{c-7D}$ (GPa)	$E_{c-28D}$ (GPa)	$E_{c-7D}/E_{c-28D}$
C0	32.3	37.2	0.87
C1	34.9	39.5	0.88
C2	38.9	39.5	0.98
C3	38.9	39.7	0.98
C4	37.2	38.1	0.98
C5	38.8	39.5	0.98
C6	33.9	34.0	1.00
C7	35.4	48.0	0.74
C8	36.9	44.8	0.82
C9	35.5	43.7	0.81

Note:  $E_{c-7D}$  =7-day elastic modulus;  $E_{c-28D}$  =28-day elastic modulus.

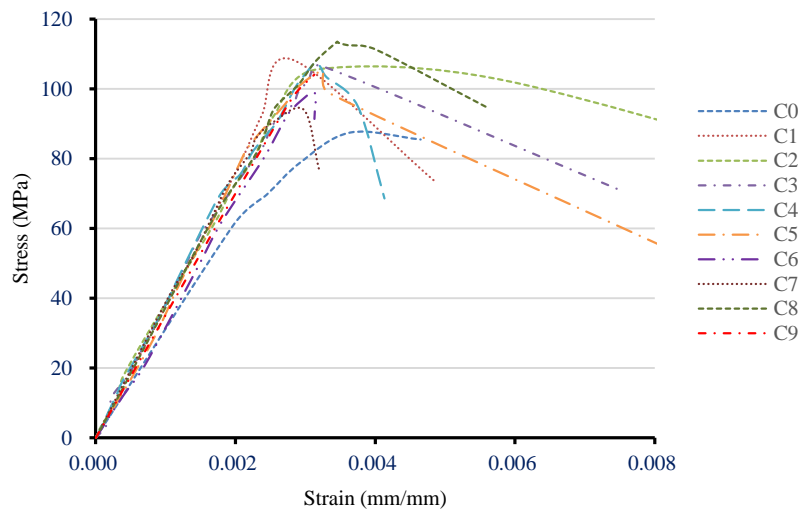


Fig. 6 Stress-strain curves of UHPC

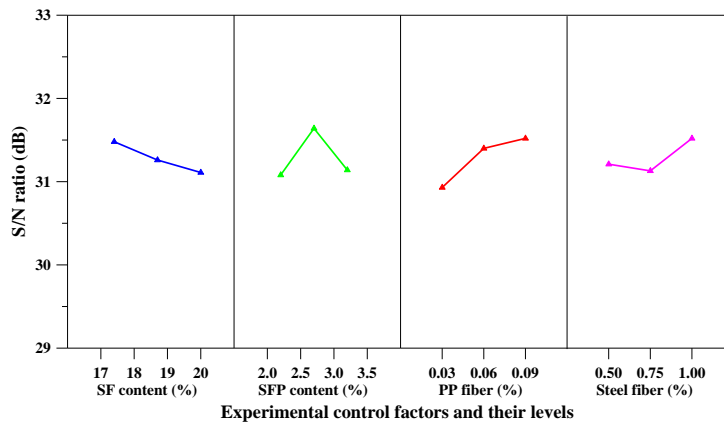


Fig. 7 S/N ratio response graph for the elastic modulus values of UHPC

### 3.2.3 Flexural strength

The load versus midspan deflection curves for each group of UHPC specimens are shown in Fig. 8. As can be seen from Fig. 8, the load-displacement curve was linear in the region before the peak point. In addition, control group exhibited brittle failure, as shown in Fig. 9(a). In contrast, all test specimens of the experimental group containing steel fiber showed greater loads and displacement capabilities than the control group. In particular, test specimens incorporating higher steel fiber content exhibited a better displacement capacity. The reason is that steel fibers have the ability to bridge cracks, as shown in Fig. 9(b). As a result, the toughness (i.e. the area under the load versus deflection curve up to fracture) of the experimental group was significantly better than that of the control group.

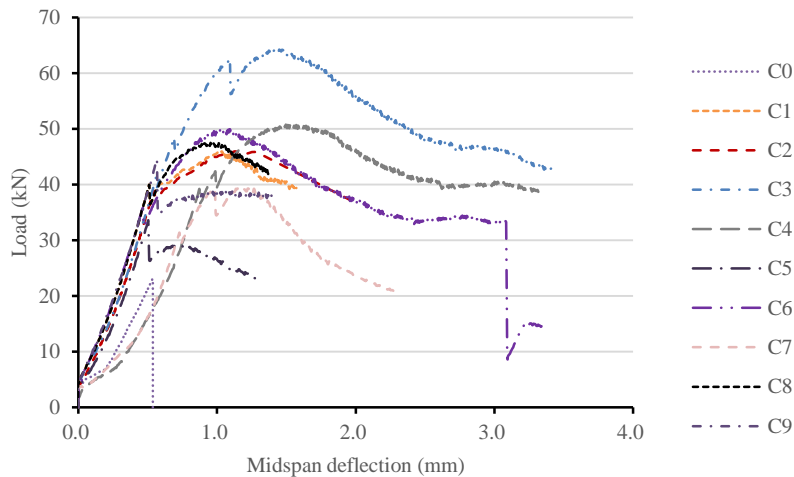
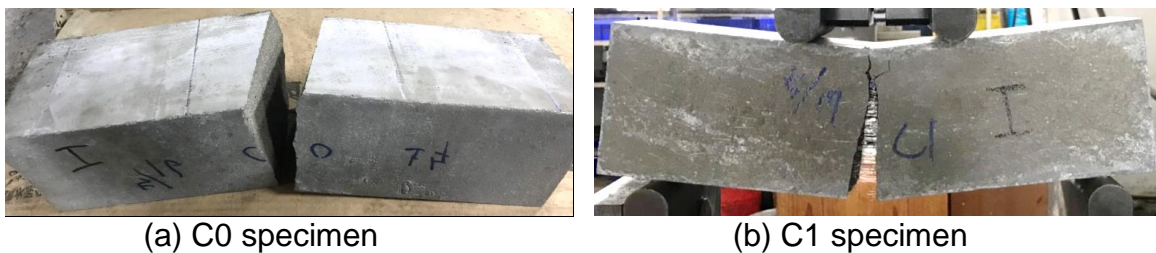


Fig. 8 Load-deflection curves of UHPC specimens



(a) C0 specimen

(b) C1 specimen

Fig. 9 Comparison of flexural test results

It can be seen from Table 10 that the 7-day flexural strength of the UHPC mixtures was between 6.6 and 18.0 MPa. Among them, the C0 mix had the lowest flexural strength (6.6 MPa), and the C3 mix had the highest flexural strength (18.0 MPa). Fig. 10 shows the *S/N* ratio response graph for 7-day flexural strength. It can be seen from Fig. 10 that as the amount of steel fiber increased, the *S/N* ratio tended to increase. According to the average *S/N* ratio of the flexural strength parameters of Table 11 and the flexural strength *S/N* response diagram of Fig. 10, the steel fiber content was an important factor affecting

the flexural strength of UHPC, and the maximum response was on the third level of the steel fiber content. Further, the results of the analysis of variance for flexural strength are given in Table 12. It can also be confirmed from Table 12 that the steel fiber content is the most important factor affecting the flexural strength of the concrete. The percentage contributions of these factors were as follows: the amount of steel fiber (42.83%) and the percentage of cement replaced by ultra-fine silica powder (37.58%). According to the analysis results of the above range analysis and variance analysis, the optimal combination level of the experimental control factors for achieving maximum flexural strength is  $A_1B_3C_2D_3$ .

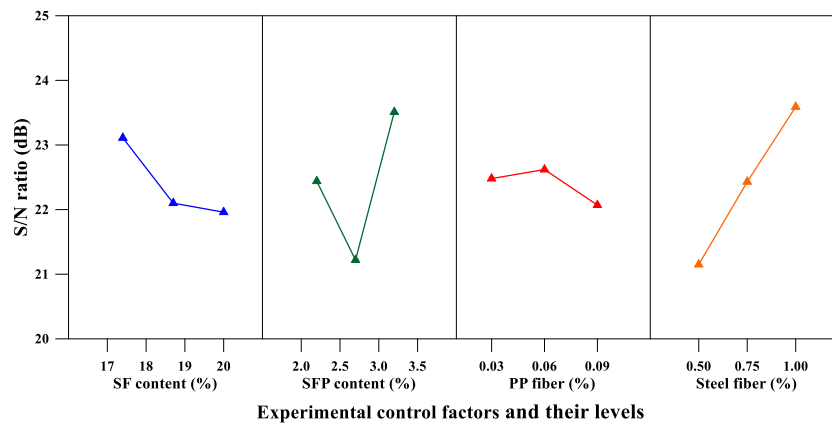


Fig. 10 S/N ratio response graph of the flexural strength values of UHPC

### 3.2.4 Splitting strength

Fig. 11 shows that the control group showed brittle failure, and the experimental group still maintained its original appearance after reaching the ultimate load, without much strain or deformation. Regarding the splitting strength of UHPC, the test results were between 4.4 and 10.8 MPa. Among them, the C0 mix had the lowest splitting strength (4.4 MPa), and the C8 mix had the highest splitting strength (10.8 MPa). Fig. 12 shows the S/N ratio response graph for 7-day splitting strength. It can be seen from Fig. 12 that as the amount of ultra-fine silica powder and steel fiber increased, the S/N ratio tended to increase. According to the average S/N ratio of the splitting strength parameters of Table 11 and the splitting strength S/N response diagram of Fig. 12, the steel fiber content was an important factor affecting the splitting strength of UHPC, and the maximum response was on the third level of the steel fiber content. Further, the results of the analysis of variance for splitting strength are given in Table 12. It can also be confirmed from Table 12 that the steel fiber content is the most important factor affecting the splitting strength of the concrete. The percentage contributions of these factors were as follows: the amount of steel fiber (45.20%) and the amount of polypropylene fiber (32.48%). According to the analysis results of the above range analysis and variance analysis, the optimal combination level of the experimental control factors for achieving maximum splitting strength is  $A_2B_3C_1D_3$ .



(a) C0 specimen



(b) C1 specimen

Fig. 11 Comparison of splitting test results

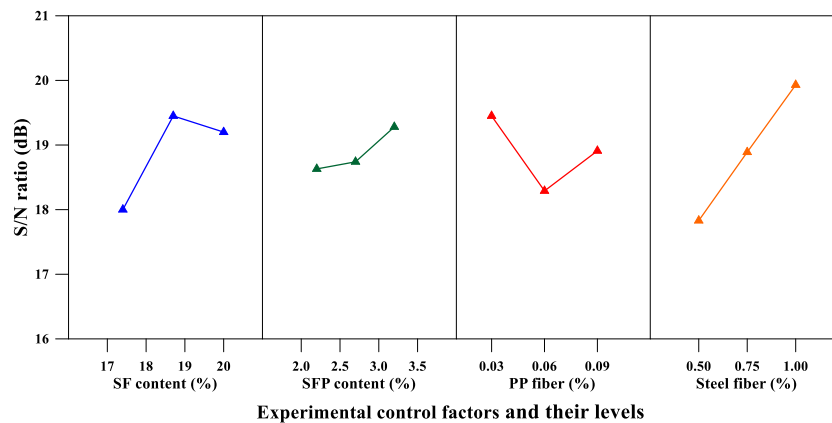


Fig. 12 S/N ratio response graph of the splitting strength values of UHPC

### 3.2.5 Confirmation test

To verify the optimal combination of the experimental control factors obtained using the Taguchi method, a confirmation test of compressive strength was performed. Table 15 shows the results of the confirmation tests. The confirmation test results show that the optimal combination of the experimental control factors proposed by the Taguchi method can obtain the maximum test results for the compressive strength performance parameter.

Table 15 Results of the confirmation test

Performance Parameter	Initial combination	Test Results (MPa)	Optimal Combination	Test Results (MPa)
Compressive Strength	A <sub>3</sub> B <sub>2</sub> C <sub>1</sub> D <sub>3</sub>	111.5	A <sub>3</sub> B <sub>2</sub> C <sub>2</sub> D <sub>3</sub>	115.7

## 4. CONCLUSIONS

The engineering properties of UHPC at early ages, including freshly mixed properties and hardened mechanical properties, have been explored in this study. Based on the above test results and analysis, the following conclusions can be obtained:

- The results show that the Taguchi method can be used to obtain suitable UHPC mix design parameters. Moreover, the confirmation test results show that the optimal

*The 2020 World Congress on  
The 2020 Structures Congress (Structures20)  
25-28, August, 2020, GECE, Seoul, Korea*

combination of the experimental control factors proposed by the Taguchi method can obtain the maximum test results for the compressive strength performance parameter.

- According to the results of the variance analysis, the amount of polypropylene fiber is the most important factor affecting the slump and slump flow of UHPC.
- The incorporation of pozzolanic materials can enhance the early-age compressive strength of UHPC, and the percentage of improvement was between 15.2% and 36.6%. Moreover, the percentage of 28-day compressive strength achieved by the UHPC mixture at seven days was between 75% and 89%.
- In the experimental group, there was no significant difference in the elastic modulus of each specimen. Moreover, the age of concrete at the time of testing was not found significantly to affect the modulus of elasticity.
- All test specimens of the experimental group containing steel fiber showed greater loads and displacement capabilities than the control group. In particular, test specimens incorporating higher steel fiber content exhibited a better displacement capacity. As a result, the toughness of the experimental group was significantly better than that of the control group.
- According to the results of the variance analysis, the steel fiber content is the most important factor affecting the splitting strength of the concrete. The percentage contributions of these factors were as follows: the amount of steel fiber (45.20%) and the amount of polypropylene fiber (32.48%).

## REFERENCES

- Abbas, S., Nehdi, M.L. and Saleem, M. A. (2016), "Ultra-High Performance Concrete: Mechanical Performance, Durability, Sustainability and Implementation Challenges", *International Journal of Concrete Structures and Materials*, **10**(3), 271-295.
- ACI Committee 239, Meeting Minutes, Toronto: *Am. Concr. Institute*, 2012.
- ACI Committee 544 (1982), "State of the art report of fiber reinforced concrete", *Concr. Int.: Des. Construct*, **4**(5), 9-30.
- Al-Manaseer, A.A. and Albert, A.J. (1995), "Measuring the consistency and workability of superplasticized concrete", *ACI Materials Journal*, **92**, 286-290.
- Alsaman, A., Dang, C.N. and Hale, W.M. (2017), "Development of ultra-high performance concrete with locally available materials", *Construction and Building Materials*, **133**, 135-145.
- ASTM C138/C138M-17a (2017), Standard Test Method for Density (Unit Weight), Yield, and Air Content (Gravimetric) of Concrete, ASTM International, West Conshohocken, PA, [www.astm.org](http://www.astm.org)
- ASTM C143/C143M-15a (2015), *Standard Test Method for Slump of Hydraulic-Cement Concrete*, ASTM International, West Conshohocken, PA, [www.astm.org](http://www.astm.org)
- ASTM C1611/C1611M-18 (2018), *Standard Test Method for Slump Flow of Self-Consolidating Concrete*, ASTM International, West Conshohocken, PA, [www.astm.org](http://www.astm.org)
- ASTM C39/C39M-18 (2018), *Standard Test Method for Compressive Strength of Cylindrical Concrete Specimens*, ASTM International, West Conshohocken, PA, [www.astm.org](http://www.astm.org)

*The 2020 World Congress on  
The 2020 Structures Congress (Structures20)  
25-28, August, 2020, GECE, Seoul, Korea*

- ASTM C469/C469M-14 (2014), *Standard Test Method for Static Modulus of Elasticity and Poisson's Ratio of Concrete in Compression*, ASTM International, West Conshohocken, PA.
- ASTM C496/C496M-11 (2004), *Standard Test Method for Splitting Tensile Strength of Cylindrical Concrete Specimens*, ASTM International, West Conshohocken, PA.
- ASTM C78/C78M-18 (2018), *Standard Test Method for Flexural Strength of Concrete (Using Simple Beam with Third-Point Loading)*, ASTM International, West Conshohocken, PA. [www.astm.org](http://www.astm.org)
- Azmeem, N.M. and Shafiq, N. (2018), "Ultra-high performance concrete: From fundamental to applications", *Case Studies in Construction Materials*, **9**, December 2018, e00197.
- Burroughs, J.F., Shannon, J., Rushing, T. S., Yi, K., Gutierrez, Q. B. and Harrelson, D.W. (2017), "Potential of finely ground limestone powder to benefit ultra-high performance concrete mixtures", *Construction and Building Materials*, **141**, 335-342.
- Erdogdu, S., Kandil, U. and Nayir, S. (2019), "Effects of cement dosage and steel fiber ratio on the mechanical properties of reactive powder concrete", *Advances in Concrete Construction*, **8**(2), 139-144. DOI: <https://doi.org/10.12989/acc.2019.8.2.139>
- Fisher, R.A. (1925), *Statistical Methods for Research Workers*, London: Oliver & Boyd.
- Ghafari, E., Arezoumandi, M., Costa, H. and Julio, E. (2015), "Influence of nano-silica addition on durability of UHPC", *Construction and Building Material*, **94**, 181-188.
- Gosavi, J.S. and Awari, U.R. (2018), "A review on high-performance concrete", *International Research Journal of Engineering and Technology (IRJET)*, **5**(5), May-2018.
- Graybeal, B. (2007), "Compressive behavior of ultra-high performance fiber-reinforced concrete", *ACI Mater. J.*, **104**(2), 146-152.
- Graybeal, B. (2014), "Ultra-high-performance concrete connections for precast concrete bridge decks", *PCI J.*, **49**(4), 48-62.
- Gu, C., Sun, W., Guo, L., Wang, Q., Liu, J., Yang, Y. and Shi, T. (2018), "Investigation of microstructural damage in ultrahigh-performance concrete under freezing-thawing action", *Advances in Materials Science and Engineering*, **2018**, Article ID 3701682, 9 pages <https://doi.org/10.1155/2018/3701682>
- He, Z.H., Du, S.G. and Chen, D. (2018), "Microstructure of ultra high performance concrete containing lithium slag", *J Hazard Mater.*, **5**(353), 35-43.
- Hughes, B.P. (1977), "Load-deflection curves for fibre-reinforced concrete beams in flexure", *Magazine of Concrete Research*, **29**(101), 199-206.
- Khaloo, A.R. and Kim, N. (1996), "Mechanical properties of normal to high-strength steel fiber-reinforced concrete", *Cem. Concr. Aggr.*, **18**(2), 92-97.
- Lai, J., Yang, H., Wang, H. and Zheng, X. (2018), "Properties and modeling of ultra-high-performance concrete subjected to multiple bullet impacts", *Journal of Materials in Civil Engineering*, **30**(10).
- Larrard, F. and Sedran, T. (1994), "Optimization of ultra-high performance concrete by the use of a packing model", *Cement and Concrete Research*, **24**, 997-1009.
- Larrard, F. and Sedran, T. (2002), "Mixture proportioning of high performance concrete", *Cement and Concrete Research*, **32**(11), 1699-1704.

*The 2020 World Congress on  
The 2020 Structures Congress (Structures20)  
25-28, August, 2020, GECE, Seoul, Korea*

- Li, P.P., Yu, Q.L. and Brouwers, H.J.H. (2018), "Effect of coarse basalt aggregates on the properties of ultra-high performance concrete (UHPC)", *Construction and Building Materials*, **170**, 649-659. DOI: 10.1016/j.conbuildmat.2018.03.109
- Metha, P.K. and Monteiro, P.J.M. (2006), *Concrete; Microstructure, Properties and Materials*, 3rd Edition, McGraw-Hill, New York.
- Mindess, S. and Bentur, A. (1983), "Concrete beams reinforced with conventional steel bars and steel fibres: properties in static loading," *The International Journal of Cement Composites and Lightweight Concrete*, **5**(3), 199-202.
- Montgomery, D.C. (2005), *Design and Analysis of Experiments*, Wiley: New York, NY, USA.
- Mosaberpanah, M.A. and Eren, O., (2018) "CO<sub>2</sub>-full factorial optimization of an ultra-high performance concrete mix design", *European Journal of Environmental and Civil Engineering*, **22**(4), 450-463, DOI: 10.1080/19648189.2016.1210030
- Myers, J.J. (1999), "How to Achieve a Higher Modulus of Elasticity", Publication – HPC Bridge Views, FHWA, Sponsored, NCBC Co-Sponsored Newsletter, **5**, 1-3.
- Nehdi, M., and Soliman, A.M. (2011), "Early-age properties of concrete: overview of fundamental concepts and state-of-the-art research", *Proc. Inst. Civ. Eng. Constr. Mater.*, **164**, 57-77.
- Neville, A.M. (1994), *Properties of Concrete*, Longman: Essex, UK.
- Okamura, H. and Ozawa, K. (1995), "Mix-design for self-compacting concrete", *Concrete Library of JSCE*, **25**, 107-120.
- Petersson, O. and Billberg, P. (1996), "A model for self-compacting concrete", *Proc. of the Int. RILEM conf. on production methods and workability of concrete*, Paisley, E&FN Spon, London, 483–492.
- Pyo, S. and Kim, H.K. (2017), "Fresh and hardened properties of ultra-high performance concrete incorporating coal bottom ash and slag powder", *Construction and Building Materials*, **131**, 459-466.
- Pyo, S., Alkaysi, M. and El-Tawil, S. (2016), "Crack propagation speed in ultra high performance concrete (UHPC)", *Construction and Building Materials*, **114**, 109-118.
- Qu, D., Cai, X. and Chang, W., (2018) "Evaluating the effects of steel fibers on mechanical properties of ultra-high performance concrete using artificial neural networks", *Appl. Sci.*, **8**(7), 1120; <https://doi.org/10.3390/app8071120>
- Rajkumar, P.R.K., Rahul, M. and Ravichandran, P.T. (2018), "Characteristic study on high performance hybrid fiber reinforced concrete using copper slag fine aggregate", *International Journal of Engineering & Technology*, **7**(2.33), 31-35.
- Sharma, R. and Bansal, P.P. (2019), "Efficacy of supplementary cementitious material and hybrid fiber to develop the ultra high performance hybrid fiber reinforced concrete", *Advances in Concrete Construction*, **8**(1), 21-31. DOI: <https://doi.org/10.12989/acc.2019.8.1.021>
- Shi, C., Wu, Z., Xiao, J., Wang, D., Huang, Z. and Fang, Z. (2015), "A review on ultra high performance concrete: part 1. raw materials and mixture design", *Construction and Building Materials*, **101**, 741-751.
- Soliman, N.A. and Tagnit-Hamou, A. (2016), "Development of ultra-high-performance concrete using glass powder–Towards ecofriendly concrete", *Construction and Building Materials*, **125**, 600-612.

*The 2020 World Congress on  
The 2020 Structures Congress (Structures20)  
25-28, August, 2020, GECE, Seoul, Korea*

- Song, P.S. and Hwang, S. (2004), "Mechanical properties of high-strength steel fiber-reinforced concrete", *Constr. Build. Mat.*, **18**, 669-673.
- Swamy, R.N. (1976), "The interfacial bond stress in steel fiber cement composites", *Cement and Concrete Research*, **6**(5), 641-650.
- Taguchi, G. (1987), *Introduction to Quality Engineering: Designing Quality into Products and Processes*, Asian Productivity Organization, Tokyo, Japan.
- Talebinejad, I., Iranmanesh, A., Bassam, S. and Shekarchizadeh, M. (2004), "Optimizing mix proportions of normal weight reactive powder concrete with strengths of 200–350 MPa", *Proceedings of the International Symposium on UHPC*, Kassel, Germany, 133-141.
- Tattersall, G.H. (1979), "Concrete: A Multi-Phase System", *Concrete*, January, 27.
- Velazco, G., Visalvanich, K. and Shah, S.P. (1980), "Fracture behavior and analysis of fiber reinforced concrete beams," *Cement and Concrete Research*, **10**(1), 41-51.
- Wille, K., Naaman, A. and Montesinos, G. (2011), "Ultra-high performance concrete with compressive strength exceeding 150 MPa (22 ksi): a simpler way", *ACI Materials Journal*, **108**(1), 46-54.
- Yu, R., Spiesz, P. and Brouwers, H. (2014), "Mix design and properties assessment of Ultra-high performance fibre reinforced concrete (UHPRFC)", *Cement and Concrete Resesearch*, **56**, 29-39.
- Zhou, Y., Xi, B., Yu, K., Sui, L. and Xing, F. (2018), "Mechanical properties of hybrid ultra-high performance engineered cementitious composites incorporating steel and polyethylene fibers", *Materials*, **11**, 1448; doi:10.3390/ma11081448.